

Vehicle motion parameter estimation using a wide-aperture acoustic sensor array of unknown shape

Kam W. Lo and Brian G. Ferguson

Maritime Operations Division, Defence Science and Technology Organisation, Sydney, Australia

ABSTRACT

A nonlinear least-squares (LS) method is formulated to estimate the speed and the closest-point-of-approach (CPA) time and range of a ground vehicle whose broadband acoustic energy emissions are received by a ground-based wide-aperture planar acoustic sensor array of unknown shape. It is assumed that the vehicle travels at a constant speed in a straight line. The three estimated motion parameters (speed, CPA time and CPA range) can be used to predict the variation with time of the vehicle range. Also, the proposed method can provide an estimate of the shape of the array if it is known on which side (left hand or right hand) the vehicle transits past the array. This passive technique is applied to real acoustic sensor data recorded during the passage of a variety of ground vehicles past a 10 m x 10 m planar cross array and its effectiveness verified by comparing the estimates with the actual values for both the vehicle motion parameters and the array sensor positions.

INTRODUCTION

Ground-based passive acoustic systems exploit the acoustic energy radiated by a source (e.g. a ground vehicle or an air vehicle) for its detection, classification, localization and tracking. As the speed of the source (assumed subsonic) is comparable with the speed of sound propagation in air, the source will have moved to a completely different position by the time its emitted acoustic signal arrives at the ground sensor. This so-called *retardation effect* complicates the solution to the problem of acoustic tracking of a manoeuvring source using bearings-only data from spatially distributed sensors (Dommermuth 1987). If the source travels at a constant velocity and a constant altitude over the time period of interest, its trajectory will be completely specified by a set of motion parameters. In this case, the retardation effect is advantageous, for it enables the estimation of some or all of the source motion parameters using a single sensor or an array of sensors (Dommermuth 1988, Dommermuth & Schiller 1984, Ferguson 1992, Ferguson & Lo 2000, Ferguson & Quinn 1994, Lo & Ferguson 2000, Lo, Ferguson, Gao & Maguer 2003, Lo, Perry & Ferguson 2002).

Lo and Ferguson (2000) described a passive acoustic technique to estimate all five motion parameters of an airborne broadband sound source using a ground-based wide-aperture acoustic sensor array. If the source is a ground vehicle, the number of motion parameters reduces to four (the height of the source is assumed to be zero). The size of the planar array is typically of order 100 m² and the motion parameter estimation method requires *a priori* knowledge of the actual shape (or relative positions of the sensor elements) of the array. Any sensor positional error will degrade the accuracy of the parameter estimates. However, it is time consuming to deploy a wide-aperture array with all sensor elements precisely located at their desired positions. Also, in practical situations where the sensor elements are deployed randomly and their positions are either unknown or crudely estimated, the motion parameter estimation method cannot be used. This paper formulates a nonlinear least-squares (LS) method to estimate three of the motion parameters of a ground vehicle using a wide-aperture planar acoustic sensor array of unknown shape.

The proposed method measures the temporal variation of the differential time-of-arrival (or time delay) of the acoustic signal at each pair of sensor elements and then minimizes the sum of the squared deviations of the noisy time delay estimates from their predicted values over a sufficiently long period of time for all sensor pairs. The vehicle's speed together with the time and range at which the vehicle is at the closest point of approach (CPA) to the array are estimated simultaneously with the shape of the array. Knowing these three motion parameters enables the range of the vehicle to be calculated as a function of time. If it is known on which side (left hand or right hand) the vehicle transits past the array, a unique estimate of the array shape can be obtained. Otherwise, there will be two possible estimates, one of them actually representing an estimate of the "mirror image" of the array shape. This passive technique is applied to real acoustic sensor data recorded in a field experiment where a variety of ground vehicles were driven past a 10 m x 10 m planar cross array at constant speeds. The estimates of the motion parameters and the sensor positions are compared with the actual values to demonstrate the accuracy of the method.

PROBLEM FORMULATION

Figure 1 shows an array of N acoustic sensors and a broadband sound source moving at a constant (subsonic) velocity v along a straight line on the XY -plane. All the N sensors are located on one side of the source trajectory. The source travels past sensor 1 at a distance d at time τ_c . The problem is to estimate the source velocity v together with the time τ_c and range d at which the source is at the CPA to sensor 1 of the array, using the received signal at each sensor, without *a priori* knowledge of the actual shape of the array. To solve this problem, a local x - y coordinate system is set up in such a way that sensor 1 is located at the origin and the x -axis is parallel to the linear trajectory of the source – see Figure 2. A (conventional) right hand coordinate system is adopted such that the *positive* y -axis intersects the source trajectory. This point of intersection is the CPA of the source to sensor 1 and its y -coordinate is equal to the CPA range d . As shown in Figure 2, if the source travels past sensor 1 on the right hand side (represented by an arrow pointing to the right), its direction of travel is in the positive x direction and the source ve-

locity v is positive; if the source travels past sensor 1 on the left hand side (represented by an arrow pointing to the left), its direction of travel is in the negative x direction and the source velocity v is negative. The source position at time τ is given by

$$x(\tau) = (\tau - \tau_c)v \quad (1)$$

$$y(\tau) = d \quad (2)$$

where $d > 0$ and $-c < v < c$ with c being the speed of sound in air.

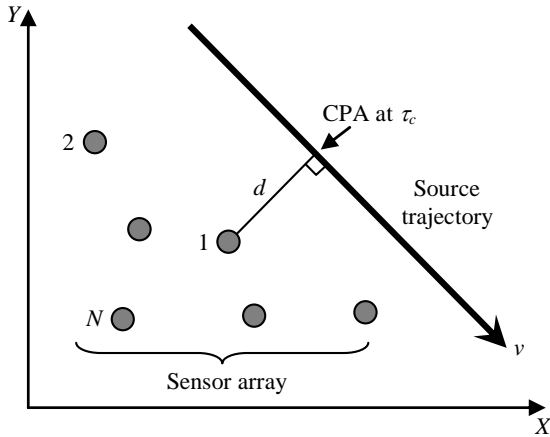


Figure 1. An array of N acoustic sensors and a broadband sound source moving at constant velocity v along a straight line on XY -plane. The source travels past sensor 1 at distance d at time τ_c .

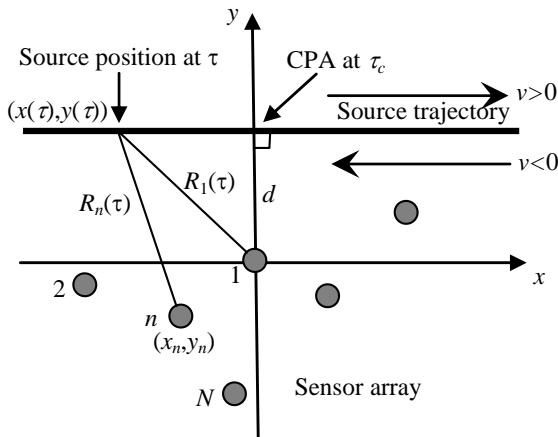


Figure 2. The sensor array and source trajectory in local x - y coordinate system.

Suppose the position of sensor n ($1 \leq n \leq N$) is given by (x_n, y_n) , with $x_1 = y_1 = 0$. (Note that the values for x_n and y_n ($2 \leq n \leq N$) vary with the direction of travel of the source on the XY -plane because the x -axis is assumed to be orientated parallel to the source trajectory.) Due to the propagation delay (commonly referred to as the *retardation effect*), the sound emitted by the source at time τ arrives at sensor n at a later time $t^{(n)}$ given by

$$t^{(n)} = \tau + R_n(\tau)/c, \quad 1 \leq n \leq N \quad (3)$$

where $R_n(\tau)$ is the radial distance to the source from sensor n at time τ , which can be expressed as

$$R_n(\tau) = \{[x(\tau) - x_n(\tau)]^2 + [y(\tau) - y_n(\tau)]^2\}^{1/2}. \quad (4)$$

The time delay β_n between sensors 1 and n at time $t = t^{(1)}$ is defined as $\beta_n(t) = t^{(n)} - t^{(1)}$. It follows from (3) that

$$\beta_n(t) = [R_n(t) - R_1(t)]/c, \quad 2 \leq n \leq N. \quad (5)$$

Substituting (1) and (2) into (4) gives

$$R_1(\tau) = [v^2(\tau - \tau_c)^2 + d^2]^{1/2} \quad (6)$$

for $n = 1$ and

$$R_n(\tau) = [R_1^2(\tau) + r_n^2 - 2dy_n - 2v(\tau - \tau_c)x_n]^{1/2} \quad (7)$$

for $2 \leq n \leq N$, where $r_n = [x_n^2 + y_n^2]^{1/2}$ is the separation distance between sensors 1 and n .

By substituting (6) into (3) (with $n = 1$), then solving the resulting equation for τ and recalling $t = t^{(1)}$, it can be shown that

$$\tau = \tau_c + \frac{c^2(t - \tau_c) - [d^2(c^2 - v^2) + v^2c^2(t - \tau_c)^2]^{1/2}}{c^2 - v^2}. \quad (8)$$

The times t and τ are referred to as the sensor (reception) time and source (emission) time respectively. Equations (5)-(8) provide an expression for $\beta_n(t)$ that is an explicit function of time t , the source velocity v , the time τ_c and range d at which the source is at the CPA to sensor 1, and the coordinates (x_n, y_n) of sensor n , for $2 \leq n \leq N$. Define the motion parameter vector $\mathbf{p} = [v, \tau_c, d]^T$, the sensor position vector $\mathbf{x} = [x_2, y_2, \dots, x_N, y_N]^T$ and the time delay vector $\mathbf{f}(t) = [\beta_2(t), \beta_3(t), \dots, \beta_N(t)]^T$, where the superscript T denotes vector transpose. The problem is now to estimate \mathbf{p} from a time series of time delay vector estimates $\{\hat{\mathbf{f}}(t_1), \hat{\mathbf{f}}(t_2), \dots, \hat{\mathbf{f}}(t_M)\}$, where $\hat{\mathbf{f}}(t_m)$ denotes the estimate of $\mathbf{f}(t)$ at time t_m for $1 \leq m \leq M$ and M is the number of estimates, without a *priori* knowledge of the actual value of \mathbf{x} . It is assumed that the observation time for $\mathbf{f}(t)$ is sufficiently long so that it encompasses both inbound (closing in range) and outbound (opening in range) legs of the vehicle transit.

ALGORITHM

This problem is solved by jointly estimating the motion parameter vector \mathbf{p} and the sensor position vector \mathbf{x} . Define the composite parameter vector $\boldsymbol{\lambda} = [\mathbf{p}^T, \mathbf{x}^T]^T$. The (nonlinear) LS estimate of $\boldsymbol{\lambda}$ is the vector $\hat{\boldsymbol{\lambda}}$ that minimizes the following cost function:

$$P(\boldsymbol{\lambda}) = \sum_{m=1}^M \|\hat{\mathbf{f}}_m - \mathbf{f}_m(\boldsymbol{\lambda})\|^2 \quad (9)$$

where $\hat{\mathbf{f}}_m \equiv \hat{\mathbf{f}}(t_m)$ is the estimated time delay vector at time t_m , $\mathbf{f}_m(\boldsymbol{\lambda}) \equiv \mathbf{f}(t_m)$ is the predicted time delay vector at time t_m , which is a function of $\boldsymbol{\lambda}$, and $\|\cdot\|$ denotes vector norm. The cost function $P(\boldsymbol{\lambda})$ is minimized using the Levenberg-Marquardt optimization algorithm (Dennis & Schnabel

1983). Denote the k th estimate of λ as $\hat{\lambda}_k$. The $k+1$ th estimate is given by:

$$\hat{\lambda}_{k+1} = \hat{\lambda}_k + (\sum_{m=1}^M \mathbf{G}_m^T \mathbf{G}_m + \mu \mathbf{I})^{-1} \times \sum_{m=1}^M \mathbf{G}_m^T [\mathbf{f}_m - \mathbf{f}_m(\hat{\lambda}_k)] \quad (10)$$

where μ is a convergence factor (Dennis & Schnabel 1983), \mathbf{I} is an $(2N+1) \times (2N+1)$ identity matrix, and \mathbf{G}_m is the $(N-1) \times (2N+1)$ Jacobian matrix evaluated at $\hat{\lambda}_k$, whose transpose is given by

$$\mathbf{G}_m^T = \nabla_{\lambda} \mathbf{f}_m^T(\hat{\lambda}_k) \quad (11)$$

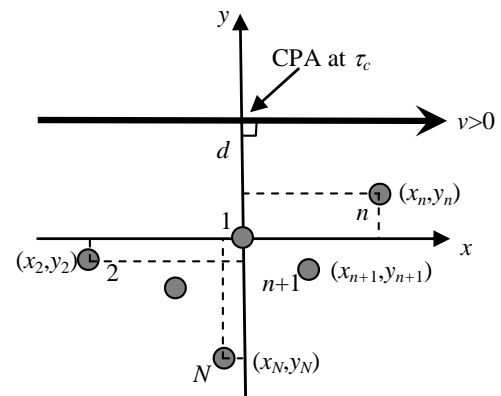
where $\nabla_{\lambda} = \left[\frac{\partial}{\partial v}, \frac{\partial}{\partial \tau_c}, \frac{\partial}{\partial d}, \frac{\partial}{\partial x_2}, \frac{\partial}{\partial y_2}, \dots, \frac{\partial}{\partial x_N}, \frac{\partial}{\partial y_N} \right]^T$ is the gradient operator. The Jacobian matrix \mathbf{G}_m can be derived using (5)-(8). The iteration (10) is repeated until $|\hat{\lambda}_{k+1} - \hat{\lambda}_k|$ is less than the specified tolerance.

AMBIGUITY IN SENSOR POSITION ESTIMATION

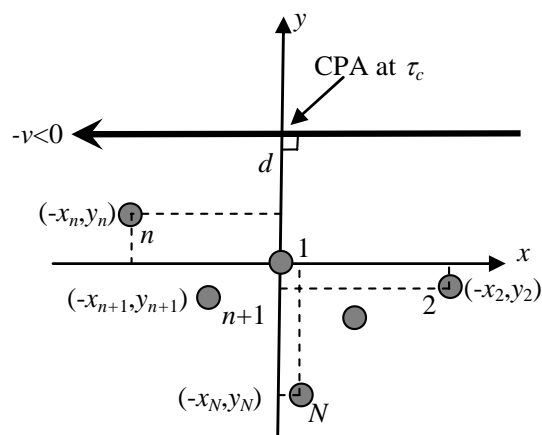
It can be verified using (5)-(8) that the same time delay vector \mathbf{f}_m can be produced by the true composite parameter vector $\lambda = [\mathbf{p}^T, \mathbf{x}^T]^T$ and a false composite parameter vector $\bar{\lambda} = [\bar{\mathbf{p}}^T, \bar{\mathbf{x}}^T]^T$, where $\bar{\mathbf{p}}$ differs from \mathbf{p} only by a sign reversal in v : $\bar{\mathbf{p}} = [-v, \tau_c, d]^T$ and $\bar{\mathbf{x}}$ from \mathbf{x} only by a sign reversal in x_n for $2 \leq n \leq N$: $\bar{\mathbf{x}} = [-x_2, y_2, \dots, -x_N, y_N]^T$. These two cases are illustrated in Figures 3(a) and (b). It is clear that $\bar{\mathbf{x}}$ is a ‘‘mirror image’’ of \mathbf{x} about the y -axis. The implication of this result is that there are two possible solutions to the minimization of the cost function $P(\lambda)$, one of them being an estimate of λ and the other an estimate of $\bar{\lambda}$.

Equation (10) will converge to either solution irrespective of the initial estimate used for λ . The correct solution can be obtained by starting the iteration with an initial estimate \hat{v}_0 of the source velocity that has the same sign as the actual source velocity, and this requires *a priori* knowledge of the side (either left hand or right hand) on which the source transits past the array. If the sign of \hat{v}_0 is correct, the iteration will produce an estimate of λ . Otherwise, the iteration will produce an estimate of $\bar{\lambda}$. However, in either case, estimates of the source speed $|v|$, CPA time τ_c and CPA range d will be obtained. These three parameter estimates can then be substituted into (6) and (8) to compute the source range $R_1(\tau)$ as a function of sensor time t . (Note that due to the signal propagation delay, the observed source range from sensor 1 at time t actually represents an estimate of the source range $R_1(\tau)$ at an earlier time τ that is related to t by (8).) Also, for the case where an estimate of λ is obtained, the source bearing $\theta(t)$ relative to the x -axis can be calculated by substituting the estimated values for v , τ_c and d into the following equation which can be derived from (1) and (2):

$$\theta(t) = \tan^{-1} \left[\frac{d}{(\tau - \tau_c)v} \right]. \quad (12)$$



(a) True solution $\lambda = [\mathbf{p}^T, \mathbf{x}^T]^T$



(b) False solution $\bar{\lambda} = [\bar{\mathbf{p}}^T, \bar{\mathbf{x}}^T]^T$

Figure 3. Ambiguity in sensor position estimation. In this illustration, (a) is the true solution and (b) the false solution. Note that the sensor positions in (b) are mirror images (about y -axis) of those in (a).

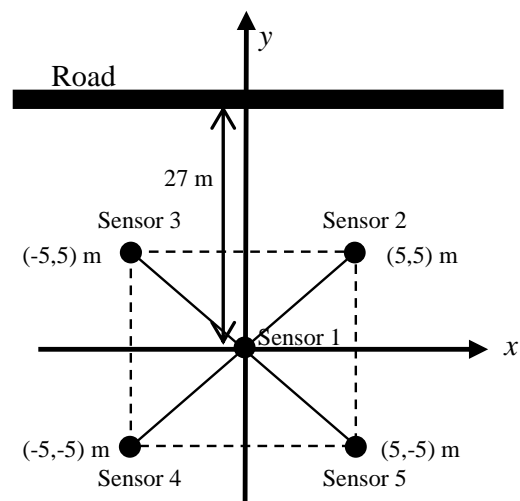


Figure 4. Geometrical configuration of five-element planar cross array. The perpendicular distance from sensor 1 to the road is 27 m.

EXPERIMENTAL RESULTS

Five microphones were located on flat ground in a cross-shaped configuration as shown in Figure 4. The perpendicular distance to the flat road from the middle sensor (sensor 1) of the array was 27 m. This is a typical setup for road monitoring. A vehicle was driven back and forth along the road many times at three different sets of speeds: slow speed (17-24 km/h), medium speed (34-46 km/h) and fast speed (47-62 km/h), and the experiment was repeated for four different types of wheeled vehicles: a commercial four-wheel drive (4WD) motor vehicle, a military 4WD motor vehicle, a medium truck, and a heavy truck. The exact numbers of transits made by each type of vehicle at the three different sets of speeds are shown in Table 1. Altogether, there were 122 vehicle transits. The acoustic data recorded from the five-element cross array were used to evaluate the proposed motion parameter estimation method.

TABLE I

Numbers of transits made by each type of vehicle at three different sets of speeds: slow, medium and fast.

| | Commercial 4WD | Military 4WD | Medium truck | Heavy Truck |
|--------|----------------|--------------|--------------|-------------|
| Slow | 11 | 6 | 10 | 12 |
| Medium | 12 | 6 | 12 | 12 |
| Fast | 13 | 5 | 12 | 11 |

The outputs of the sensors were sampled at 1 kHz. The data from each sensor were processed in non-overlapped blocks, each containing 256 samples. Each data block from sensor 1 was cross-correlated with the corresponding data block from each of the other sensors. The phase transform prefiltering technique was used to suppress ambiguous peaks which would otherwise have appeared in the cross-correlation function due to the strong harmonic components of the source signal. The generalized cross-correlation processing (with phase transform prefiltering) was implemented in the frequency domain using the fast Fourier transform, with a rectangular spectral window from 10 to 300 Hz where the signal-to-noise ratio was observed to be high. The peak of the generalized cross-correlation function was refined using a 3-point quadratic interpolation, and the position along the lag axis of the refined peak gives the time delay estimate.

Figure 5 shows, as dots, the estimated time delays for the four sensor pairs as functions of sensor time for a particular vehicle transit. The LS estimate of λ corresponds to the vector $\hat{\lambda}$ that provides a LS fit of the time delay model to the temporal sequences of time delay estimates for the four sensor pairs. An initial estimate $\hat{\lambda}_o$ was obtained as follows. The initial estimates of the x and y coordinates of each sensor were set arbitrarily to zero. The initial estimate \hat{d}_o of the CPA range was set equal to 100 m. Knowing that sensor 2 was located on the right hand side and sensor 3 on the left hand side of sensor 1, the direction of travel of the vehicle along the road (either from left to right or from right to left) could be derived from the temporal variation of the time delay for sensors 2 and 3. Using this information the correct sign was determined for the initial estimate \hat{v}_o of the source velocity, whose magnitude was set equal to 100 km/h. A correct sign for \hat{v}_o ensured that the shape of the array (not its mirror image) was estimated along with the vehicle's three motion parameters. The sensor CPA time t_c is related to the source CPA time τ_c by $t_c = \tau_c + d/c$. An initial estimate

$\hat{t}_{c,o}$ of t_c was obtained by finding the time when the received signal energy at sensor 1 attained its maximum. An initial estimate $\hat{\tau}_{c,o}$ of τ_c was then calculated as $\hat{\tau}_{c,o} = \hat{t}_{c,o} - \hat{d}_o/c$. The observation time for the time delay vector $\mathbf{f}(t)$ was 10 s centred at $\hat{t}_{c,o}$. All the time delay estimates $\hat{\mathbf{f}}_m$ within this time interval were used in (10) to compute the LS estimate of λ iteratively with $\hat{\lambda}_o$ being the initial estimate. An improved estimate of t_c was then computed as $\hat{t}_c = \hat{\tau}_c + \hat{d}/c$, where $\hat{\tau}_c$ and \hat{d} are the current LS estimates of the CPA time and CPA range respectively. The parameter estimation was repeated by centering the observation time of 10 s for $\mathbf{f}(t)$ at \hat{t}_c . However, this time, the iteration of (10) was started with the current LS estimate of λ .

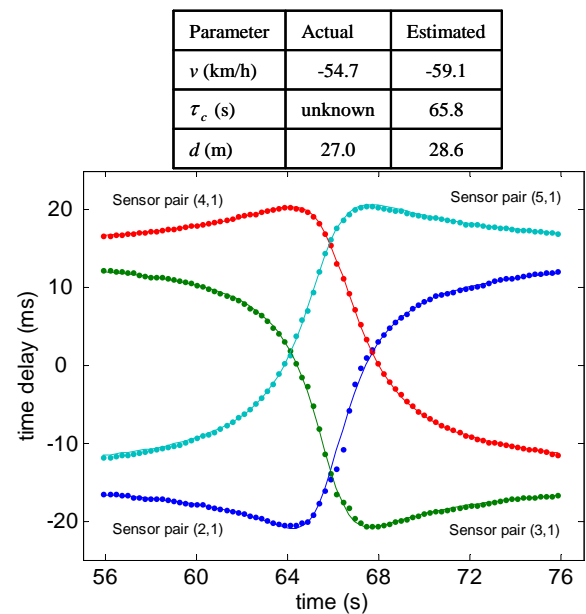


Figure 5. Time delays for the four sensor pairs as functions of sensor time for a particular vehicle transit. Estimated values (dots). LS fit (solid lines).

The solid curves in Figure 5 represent the LS fit of the time delay model to the temporal sequences of time delay estimates for the four sensor pairs. The actual and estimated values of the vehicle's three motion parameters are shown on the top of Figure 5. The variations with sensor time of the range and bearing of the vehicle were predicted using the estimated motion parameters and the results are shown in Figures 6(a) and (b) respectively. Also included in these figures for comparison are the range and bearing estimates obtained using the source localization method described by Lo & Ferguson (2000) that requires *a priori* knowledge of the array shape. This method of source localization is based on the curvature of the incident wavefront of the acoustic signal and estimates the instantaneous source position using time delay measurements for the four sensor pairs of the planar cross array. Its ranging accuracy, as observed from Figure 6(a), degrades rapidly with range exceeding a value (100 m) that is 10 times the length or width (10 m) of the planar array. (A similar result has been observed when using a wavefront curvature technique to locate broadband sound sources with a linear array of three equally spaced sensors (Ferguson 2000).)

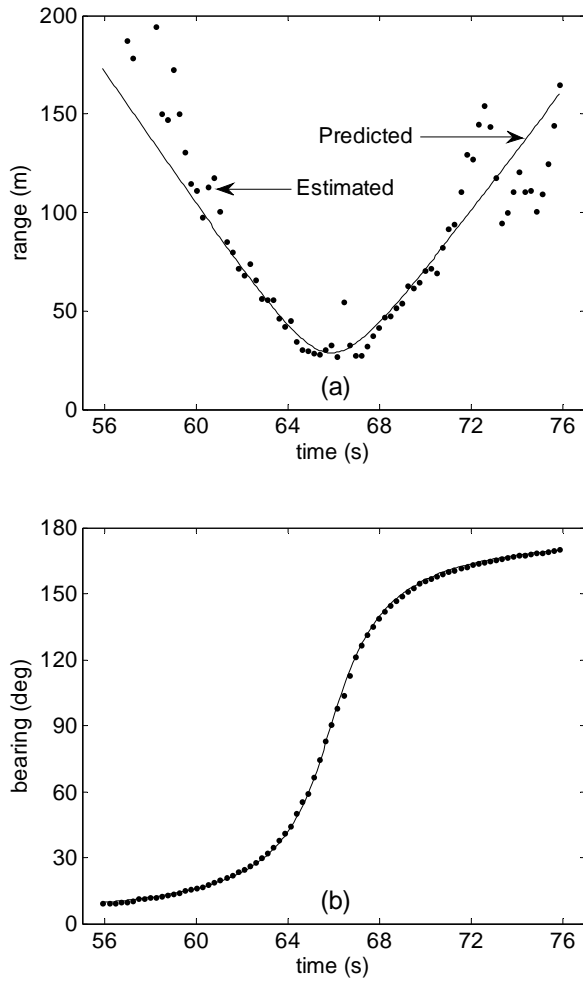


Figure 6. (a) Range and (b) bearing of vehicle versus sensor time. Predicted values (solid line) using the estimated motion parameters. Estimated values (dots) using the source localization method described by Lo & Ferguson (2000).

Figure 7 shows the estimated positions of sensors 2 to 5 for all 122 vehicle transits. The actual positions of the four sensors coincide with the four corners of the square. The bias errors and standard deviations in the estimated x and y coordinates for each sensor are shown in Figure 8. The radial bias and circular error probable (CEP) for each of the four sensors were computed using the estimated x and y coordinates of the sensor for all 122 vehicle transits and the results are shown in Figure 9. (The CEP is a measure of the uncertainty in the location estimate $\hat{\mathbf{x}}_n$ of a sensor relative to its mean $E[\hat{\mathbf{x}}_n]$, where $E[\cdot]$ denotes the expected value of the quantity in brackets. The CEP is defined as the radius of the circle centred at $E[\hat{\mathbf{x}}_n]$ and containing a specified percentage of the realizations of $\hat{\mathbf{x}}_n$. For example, the 50% CEP contains half of the realizations of $\hat{\mathbf{x}}_n$. The radial bias is the separation distance between the mean location estimate $E[\hat{\mathbf{x}}_n]$ and the actual position \mathbf{x}_n of a sensor.)

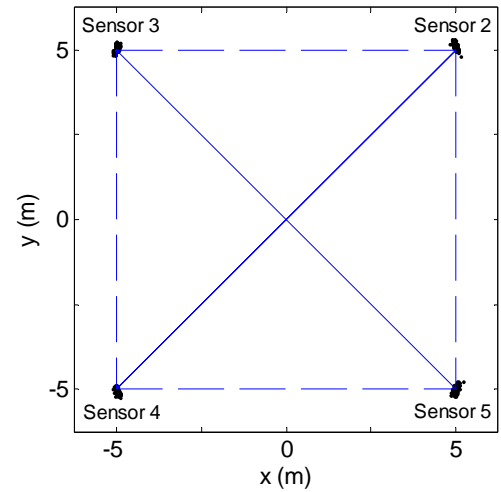


Figure 7. Estimated positions of sensors 2 to 5 for all 122 vehicle transits. The actual sensor positions correspond to the four corners of the square.

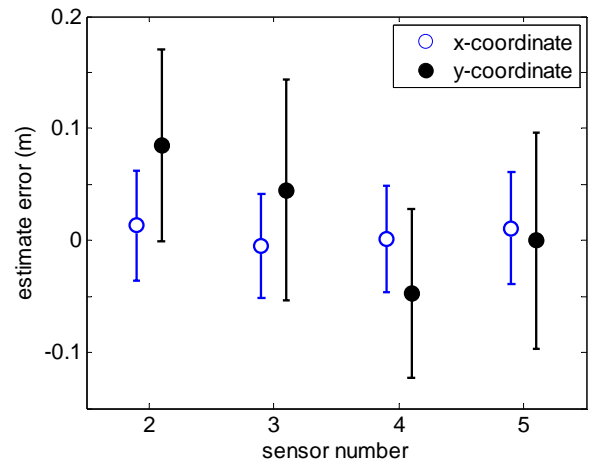


Figure 8. Bias errors in estimated x and y coordinates for sensors 2 to 5. The error bars represent one standard deviation.

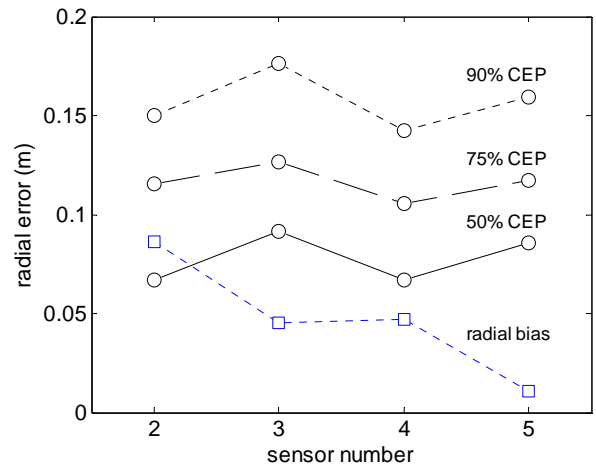


Figure 9. Radial bias errors and CEPs for sensors 2 to 5.

The cumulative probability distributions (CPDs) of the relative errors in the speed and CPA range estimates were computed using the estimated values of these two parameters for all 122 vehicle transits, and the results are shown in Figures 10(a) and (b) respectively. (The CPD of a relative error at ε is the probability that the magnitude of the relative error is less than or equal to ε .) The corresponding results for a similar time-delay based motion parameter estimation method (Lo & Ferguson 2000) but requiring *a priori* knowledge of the array shape are also included in Figures 10(a) and (b) for comparison.

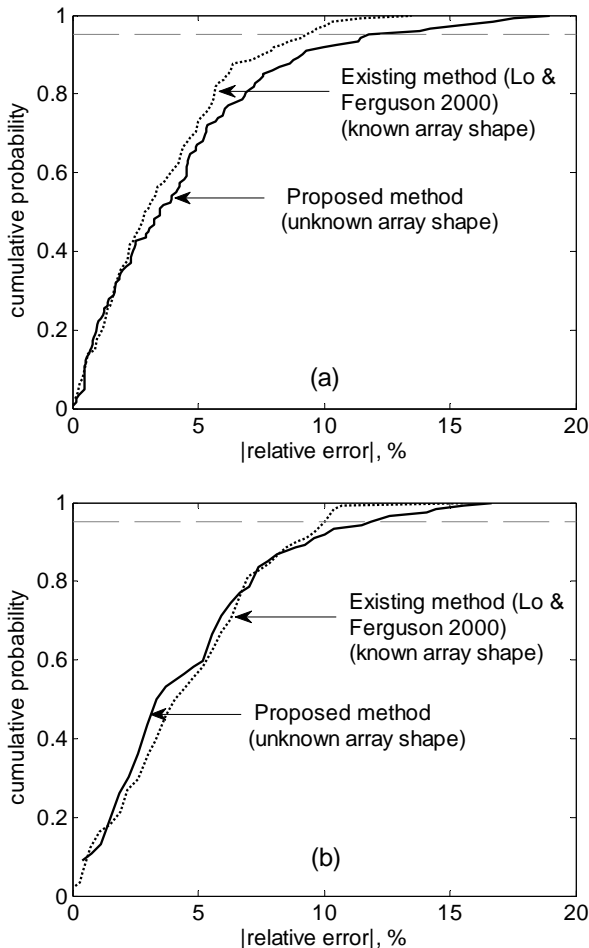


Figure 10. CPDs of relative errors in (a) speed and (b) CPA range estimates.

CONCLUSIONS

A nonlinear LS method has been formulated to estimate three of the motion parameters of a ground vehicle whose broadband acoustic energy emissions are received by a ground-based wide-aperture planar acoustic sensor array of unknown shape. Field experiment results show that the method provides reliable estimates of the speed and CPA range of the vehicle. For example, the probabilities that the relative errors in the speed and CPA range estimates are less than or equal to 10% are both higher than 0.91. The proposed method estimates the motion parameters simultaneously with the array shape, with an accuracy that is only slightly worse than that of the existing method (Lo & Ferguson 2000) where the sensor positions are known. Specifically, for a cumulative probability of 0.95, the relative errors in the speed and CPA range estimates for the proposed method are (respectively) about 2.5% and 1.8% larger than those for the existing method.

Once the estimates of the vehicle's speed, CPA time and CPA range are obtained, the range of the vehicle can be calculated as a function of time.

If it is known on which (left or right) side the vehicle transits past the array, the proposed method is able to provide a good estimate of the array shape as demonstrated by the experimental result. The biased errors in the estimated x and y coordinates for each of the four sensors are less than 1 cm and 9 cm (0.1% and 0.9% of the width of the planar array) respectively, and the corresponding standard deviations are less than 5 cm and 10 cm (0.5% and 1% of the width of the planar array) respectively. To estimate the absolute (global) positions of the sensors (on the XY -plane) would require a knowledge of the orientation of the array (or the direction of travel of the vehicle) and the absolute position of sensor 1.

ACKNOWLEDGMENT

This research is in support of DSTO's Automation of the Battlespace Initiative.

REFERENCES

- Dennis, JE & Schnabel, RB 1983, *Numerical methods for unconstrained optimization and nonlinear equations*, Englewood Cliffs, NJ: Prentice-Hall.
- Dommermuth, F 1988, 'The estimation of target motion parameters from cpa time measurements in a field of acoustic sensors', *J. Acoust. Soc. Am.*, vol. 83, no. 4, pp. 1476-1480.
- Dommermuth, FM 1987, 'A simple procedure for tracking fast maneuvering aircraft using spatially distributed acoustic sensor', *J. Acoust. Soc. Am.*, vol. 82, no. 4, pp. 1418-1424.
- Dommermuth, F & Schiller, J 1984, 'Estimating the trajectory of an accelerationless aircraft by means of a stationary acoustic sensor', *J. Acoust. Soc. Am.*, vol. 76, no. 4, pp. 1114-1122.
- Ferguson, BG 1992, 'A ground-based narrow-band passive acoustic technique for estimating the altitude and speed of a propeller-driven aircraft', *J. Acoust. Soc. Am.*, vol. 92, pp. 1403-1407.
- Ferguson, BG 2000, 'Variability in the passive ranging of acoustic sources in air using a wavefront curvature technique', *J. Acoust. Soc. Am.*, vol. 108, no. 4, pp. 1535-1544.
- Ferguson, BG & Lo, KW 2000, 'Turboprop and rotary-wing aircraft flight parameter estimation using both narrow-band and broadband passive acoustic signal-processing methods', *J. Acoust. Soc. Am.*, vol. 108, no. 4, pp. 1763-1771.
- Ferguson, BG & Quinn, BG 1994, 'Application of the short-time Fourier transform and the Wigner-Ville distribution to the acoustic localization of aircraft', *J. Acoust. Soc. Am.*, vol. 96, no. 2, Pt. 1, pp. 821-827.
- Lo, KW & Ferguson, BG 2000, 'Broadband passive acoustic technique for target motion parameter estimation', *IEEE Trans. Aerosp. Electron. Syst.*, vol. 36, no. 1, pp. 163-175.
- Lo, KW, Ferguson, BG, Gao, Y & Maguer, A 2003, 'Aircraft flight parameter estimation using acoustic multipath delays', *IEEE Trans. Aerosp. Electron. Syst.*, vol. 39, no. 1, pp. 259-268.
- Lo, KW, Perry, SW & Ferguson, BG 2002, 'Aircraft flight parameter estimation using acoustical Lloyd's mirror effect', *IEEE Trans. Aerosp. Electron. Syst.*, vol. 38, no. 1, pp. 137-150.